Chaotic Stokes flow in 3D granular porous media and its impact on solute mixing

Yves Méheust
yves.meheust@univ-rennes1.fr

Geosciences Department (UMR CNRS 6118)
Sciences of the Universe Observatory
University of Rennes
Rennes (France)

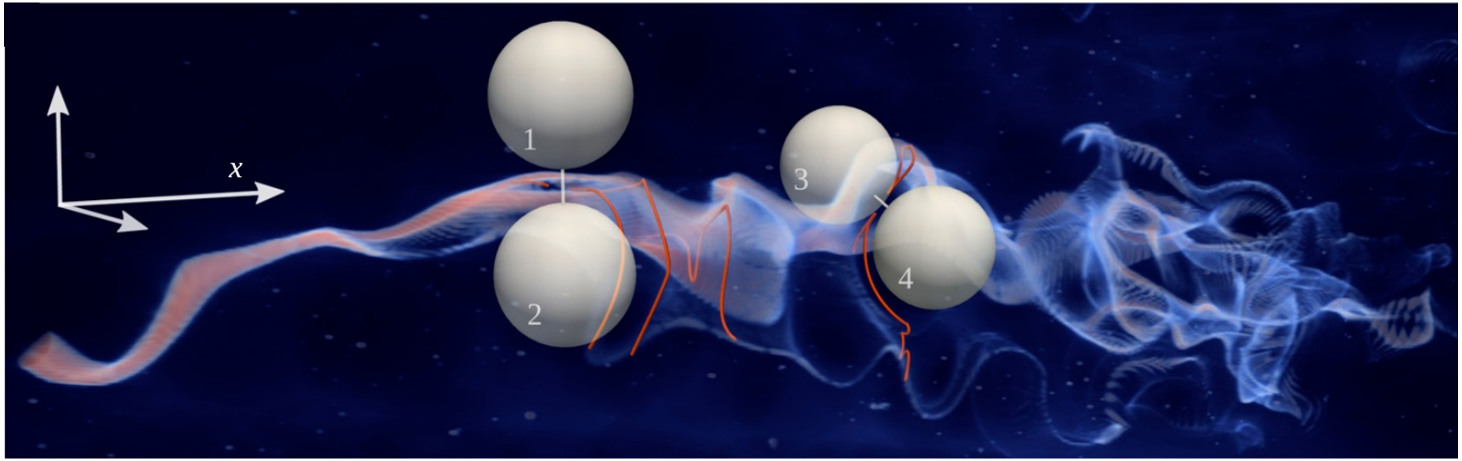

Our study objects: subsurface porous media

Porous media = solid materials with connected cavities allowing fluid flow

Continous porous media

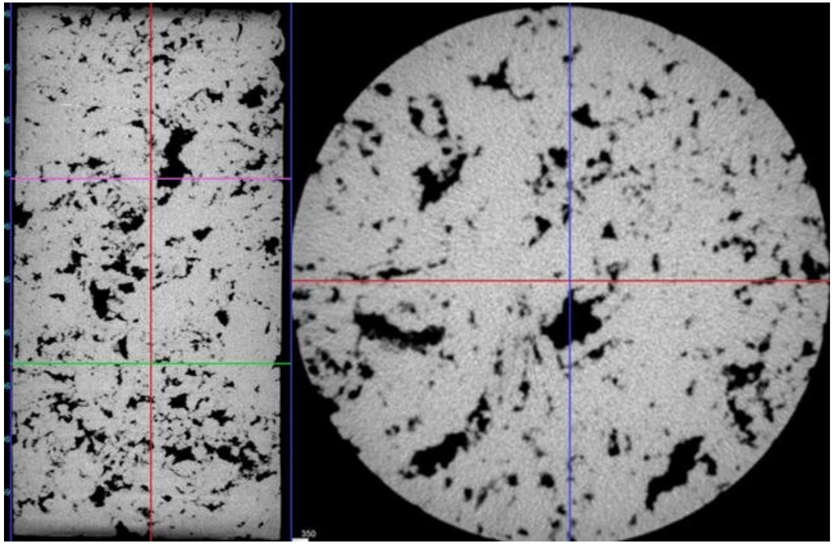

Carbonate (oil reservoir)

Granular porous media

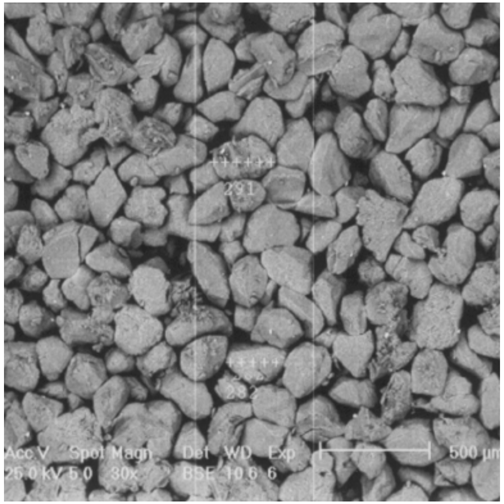

Sandstone (deep aquifer)

Glass beads

We shall consider saturated porous media → only one aqueous fluide phase

Solute transport and solute mixing

Solute transport:

- Advection displaces the solutes with the local flow velocity
- Molecular diffusion tends to homogenize the solutes' concentration fields

Péclet number: $$Pe = \frac{t_{\mathrm{diff}}}{t_{\mathrm{adv}}} = \frac{U\,L}{D_{\mathrm{m}}}$$

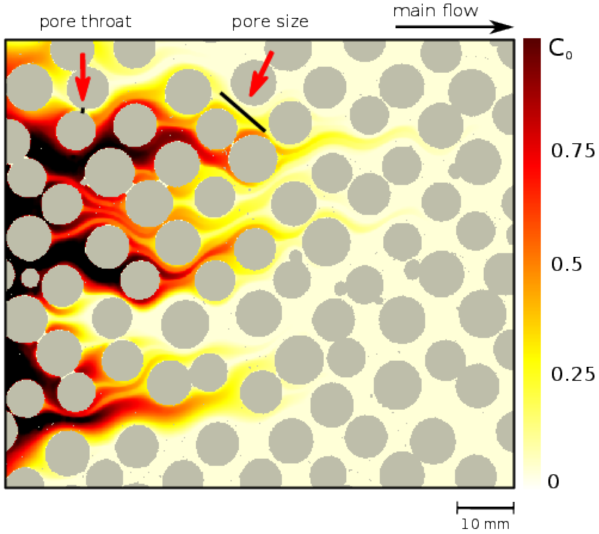

Solute mixing = evolution of the concentration fields towards homogeneity

→ characterized by the time evolution of the concentration PDF

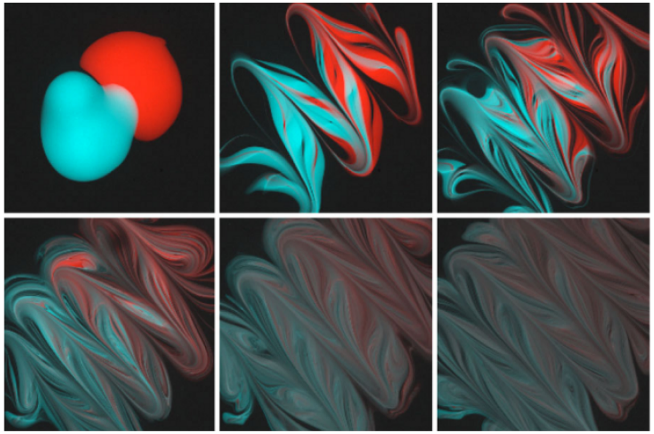

Duplat et al.
PRL (2010)

→ Controls effective reaction rates at large Damköhler numbers

Solute transport and mixing in subsurface water

Clogging of geothermal fields by biofilms

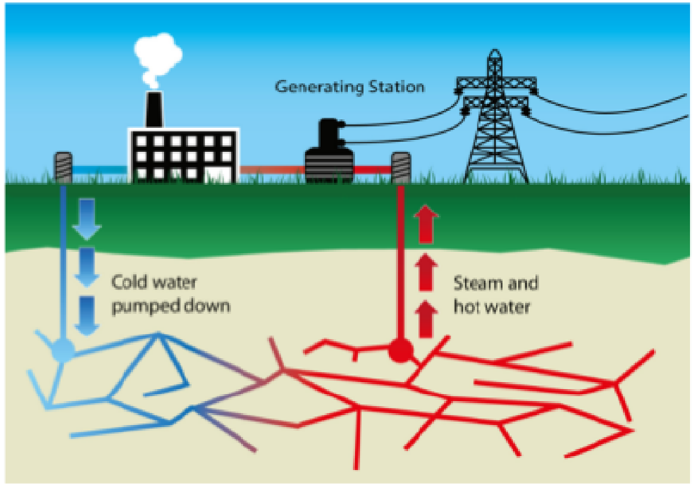

Subsurface remediation

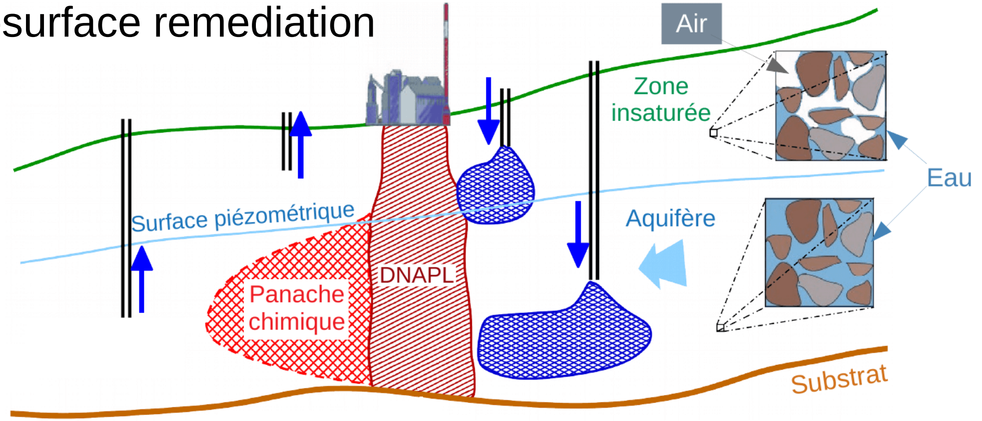

CO₂ storage

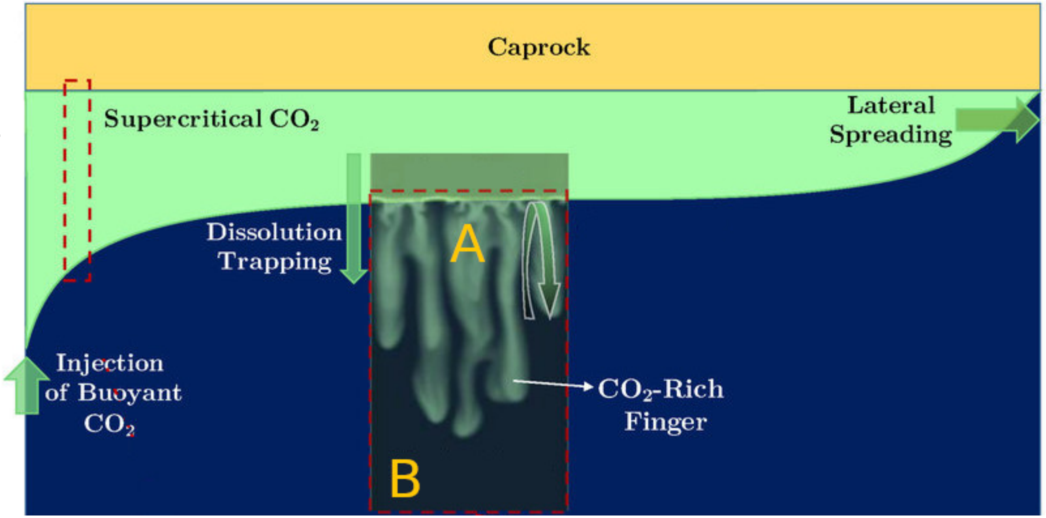

And also:

- Nutrient landscapes for bacteria in soils
- Chemical processes in packed bed reactors
- Chemical processes in batteries

The advective solute “backbone” → lamellar theory of mixing

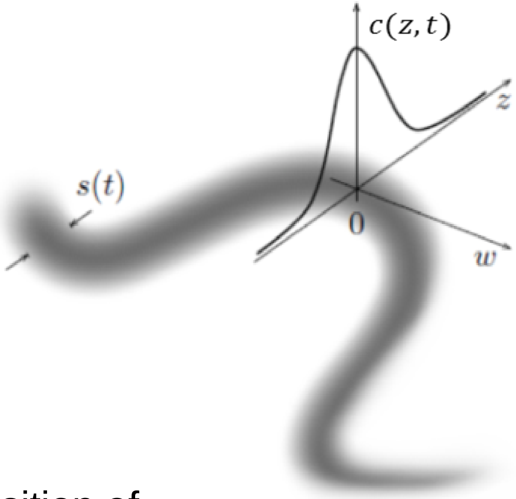

A finite mass of solute is stretched into a filament by the heterogeneous flow:

For an infinitesimal length of the filament (the lamella), transverse compression due to longitudinal stretching competes with molecular diffusion:

$$\frac{1}{s(t)}\frac{ds}{dt} = \frac{D_{\text{eff}}}{s(t)^2} - \frac{1}{l(t)}\frac{dl}{dt}$$

(compression-diffusion equation)

Ranz, AIChE J. (1979); Villermaux & Duplat, PRL (2003)

At sufficiently large Péclet, the time evolution of the filament/plume is the superposition of

- The displacement of the advective backbone of the filament, and its elongation/compression
- The diffusive widening of that filament

→ The advective backbone plays a critical role in term of controlling the stretching law

→ “Chaotic mixing” = chaotic advection = chaotic mixing at very high Péclet

Chaotic advection in continuous porous media

Analytical/numerical study of purely advective transport in synthetic continuous porous media:

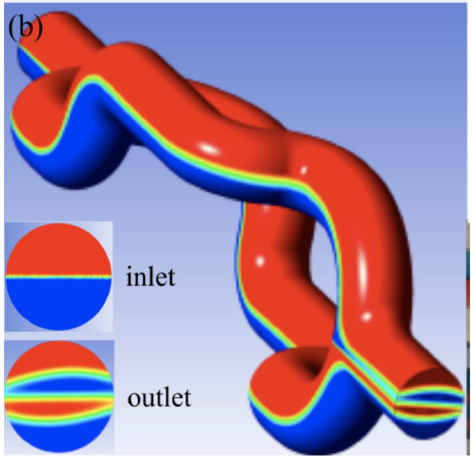

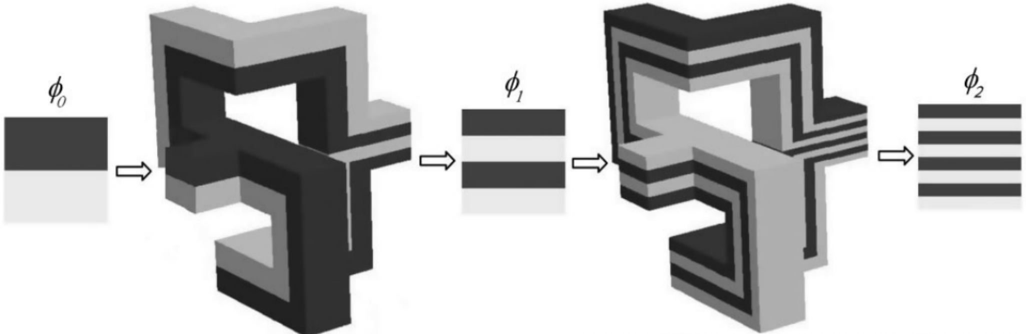

“Baker’s map”

Lester et al.
(PRL 2013, AWR 2016)

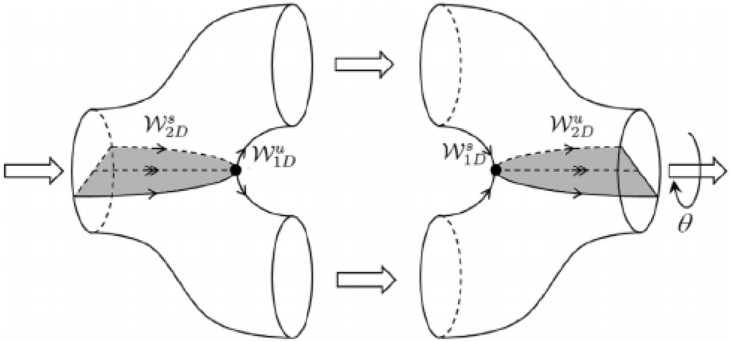

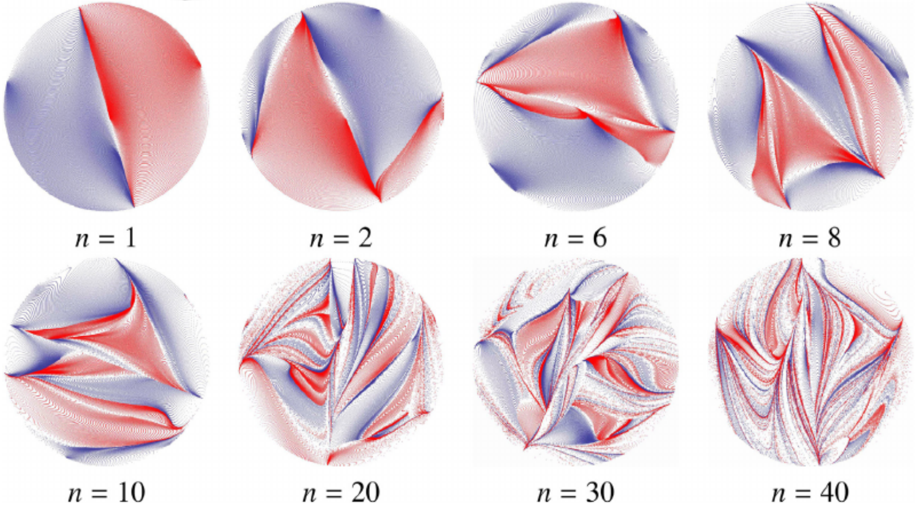

→ Exponential growth of the interface’s length → Intrinsically chaotic flow in random media

- Is this still true in granular porous media ?
- Is randomness a necessary feature ?

1) Chaotic advection in a regular packing of monodisperse beads: A numerical study

Stokes flow simulation in ordered packings of monodisperse beads

Simple cubic lattice

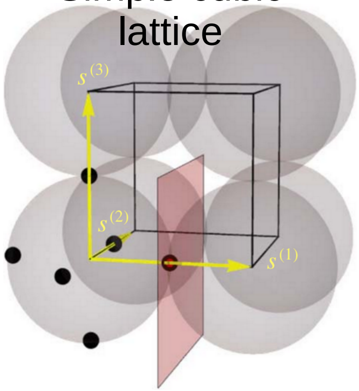

Body-centered cubic lattice

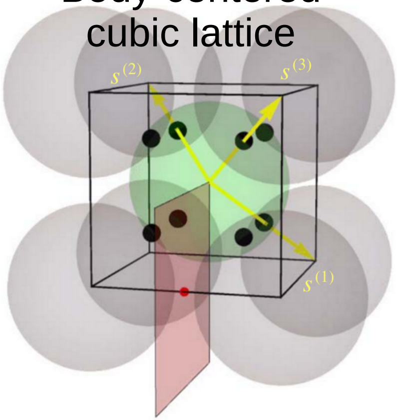

Turuban et al., PRL (2018)

3D Stokes ($Re \ll 1$) along a mean flow direction $\boldsymbol{q} \equiv \frac{1}{|\langle \boldsymbol{v} \rangle|} \langle \boldsymbol{v} \rangle$

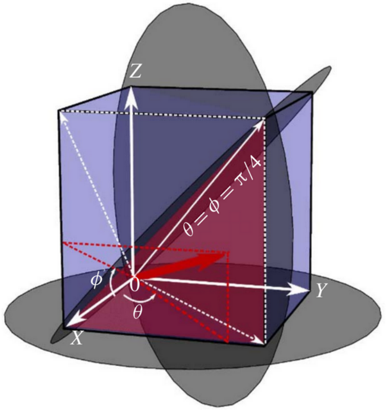

Orientational space:

$$\mathcal{H} : (\phi, \theta) = [0, \pi/4] \times [0, \pi/4]$$

Trajectories for the BCC lattice:

$$(\theta_f, \phi_f) = (\pi/40, 7\pi/90)$$

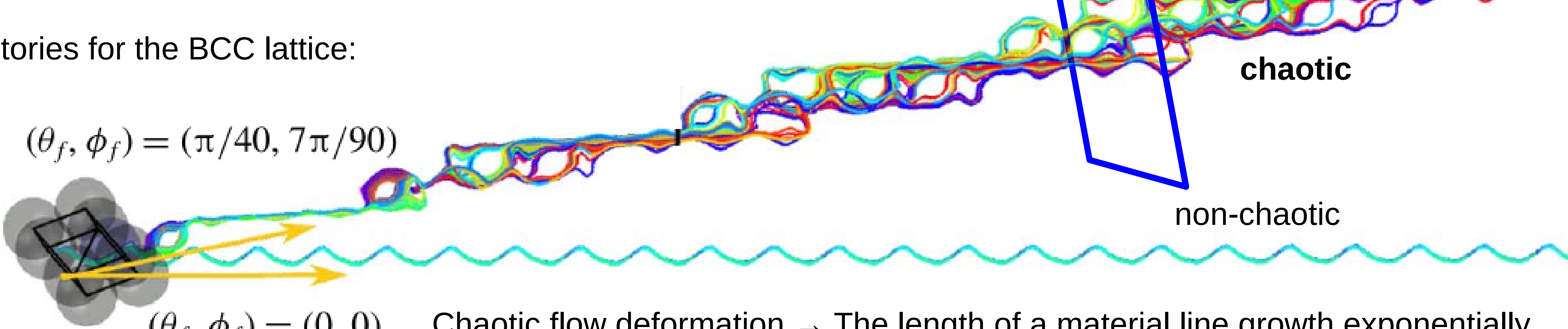

chaotic

non-chaotic

$$(\theta_f, \phi_f) = (0, 0)$$

Chaotic flow deformation → The length of a material line growth exponentially

Quantitative characterization of the chaotic behavior

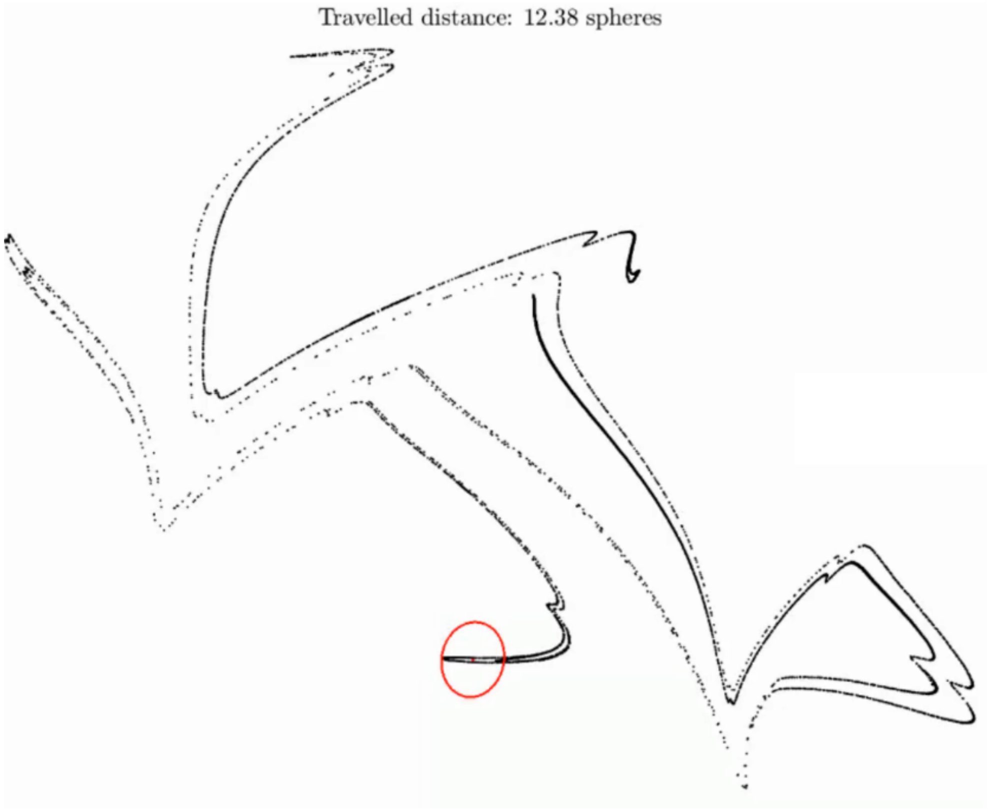

Turuban et al., PRL (2018)

Exponential growth in time in a finite space

→ Material lines have have to fold periodically

Lyapunov exponent = scalar measure of the logarithmic growth rate of the length of material lines

Cauchy-Green tensor:

$\mathbf{C}(\mathbf{X}, t) = \mathbf{F}^\top \cdot \mathbf{F}$ $\mathbf{F}$ = rate of deformation tensor

$\nu(t)$ = largest eigenvalue of the Cauchy-Green tensor

Lyapunov exponent: $\boxed{\lambda \equiv \lim_{t\to\infty} \frac{\ell}{2s(t)} \ln[\nu(t)]}$

ℓ = unit cell length

$s(t) \equiv \mathbf{q} \cdot (\mathbf{x}(t) - \mathbf{x}(0))/|\mathbf{q}|$ = longitudinal distance traveled

Dependence of the Lyapunov exponent on the mean flow orientation

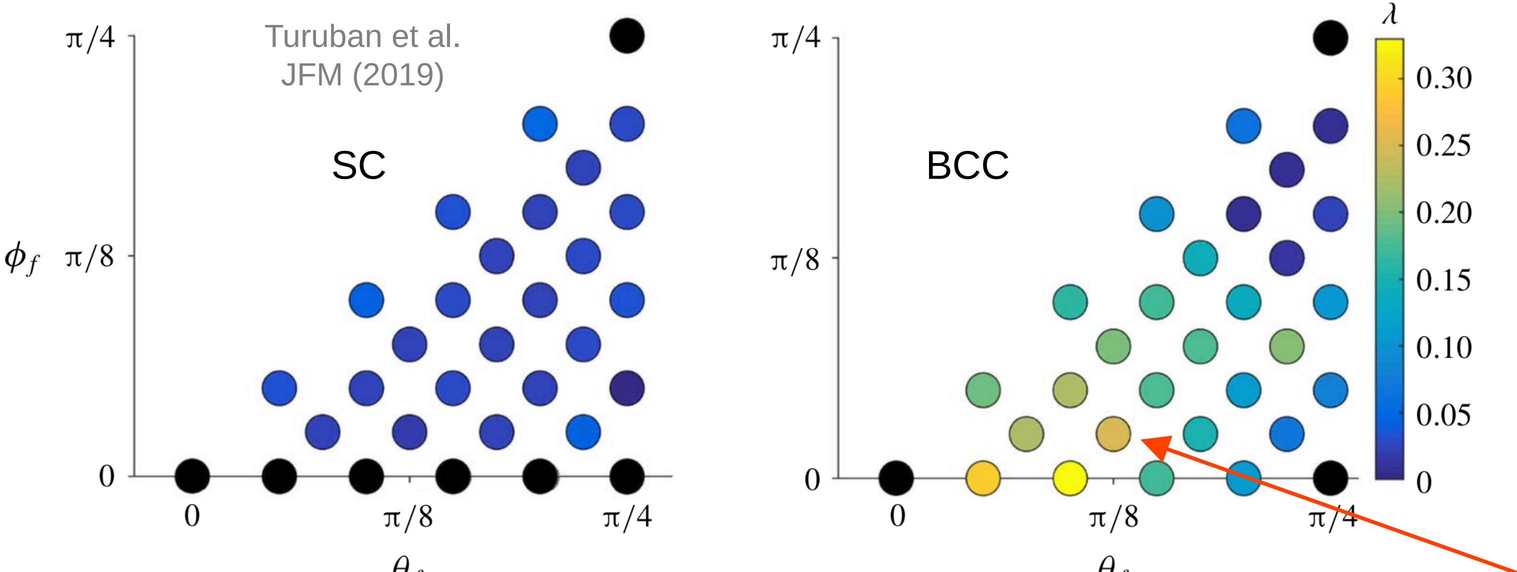

The Lyapunov is 0 if the mean flow direction is normal to a reflection symmetry plane of the lattice

Associated Poincaré sections for the BCC lattice:

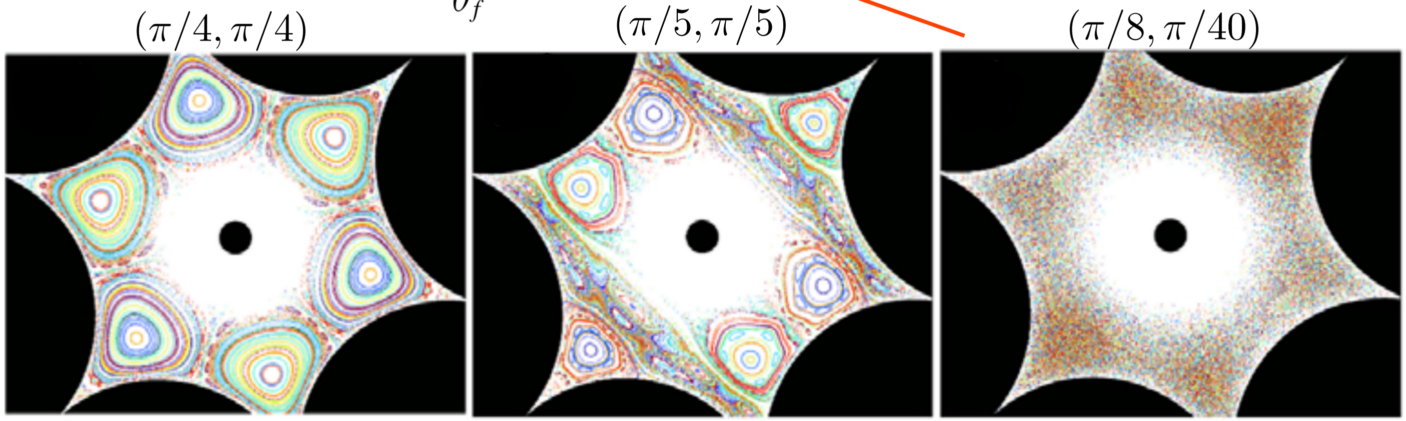

Where does chaos originate from ? – Stable and unstable 2D manifolds

Streamlines around a spherical grains for a single sphere and for a sphere positioned among other spheres:

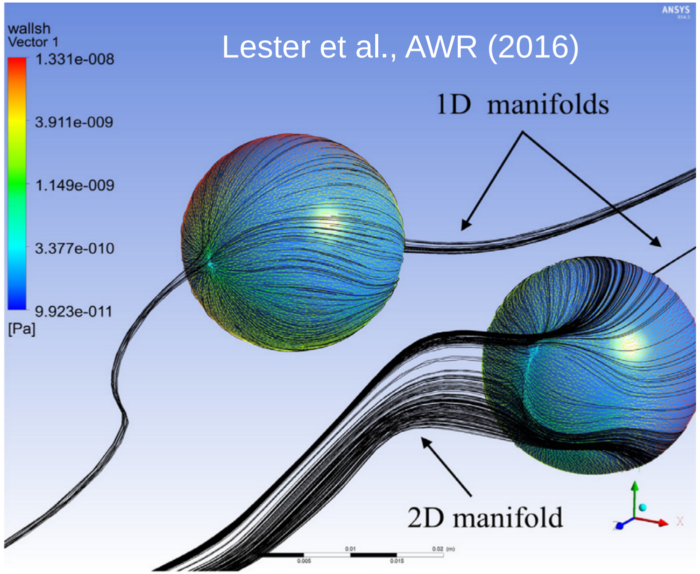

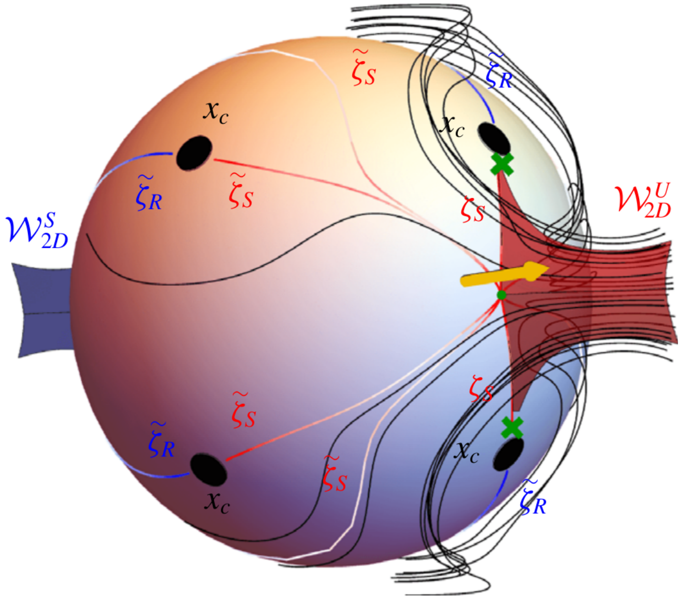

Stable and unstable 2D manifolds = separation and reattachment surfaces that undergo exponential contraction and stretching (respectively)

Turuban et al.
(PRL, 2018, JFM 2019)

Where does chaos originate from ? – Stable and unstable 2D manifolds

Streamlines around a spherical grains for a single sphere and for a sphere positioned among other spheres:

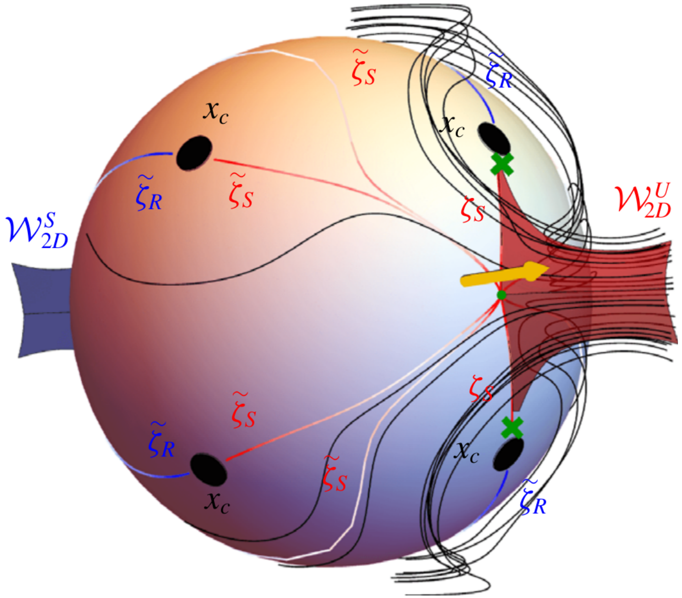

The topology of the skin friction controls the origin of manifolds at the grains' surfaces:

Skin friction field: $\boldsymbol{u}\left(x_1, x_2\right) \equiv \left.\frac{\partial \boldsymbol{v}}{\partial x_3}\right|_{x_3=0}$

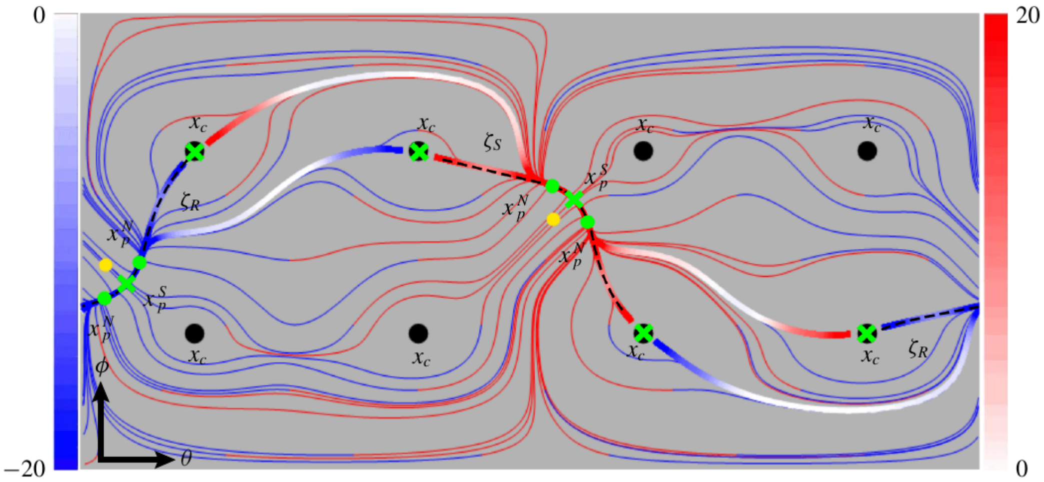

Stable and unstable 2D manifolds = separation and reattachment surfaces that undergo exponential contraction and stretching (respectively)

Turuban et al.
(PRL, 2018, JFM 2019)

Critical points: $\boldsymbol{u}\left(\boldsymbol{x}_p\right) = \boldsymbol{0}$

→ Classified according to the eigenvalues of the skin friction tensor $\boldsymbol{A} \equiv \left.\frac{\partial \boldsymbol{u}}{\partial \boldsymbol{x}}\right|_{\boldsymbol{x}=\boldsymbol{x}_p}$

Where does chaos originate from ? – Intersections between manifolds

Smooth intersection between a stable and an unstable manifold originating from different grains:

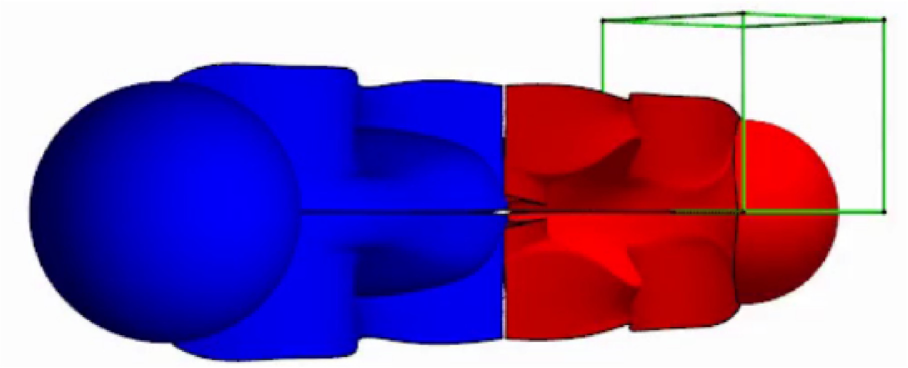

Transverse intersection between a stable and an unstable manifold originating from different grains:

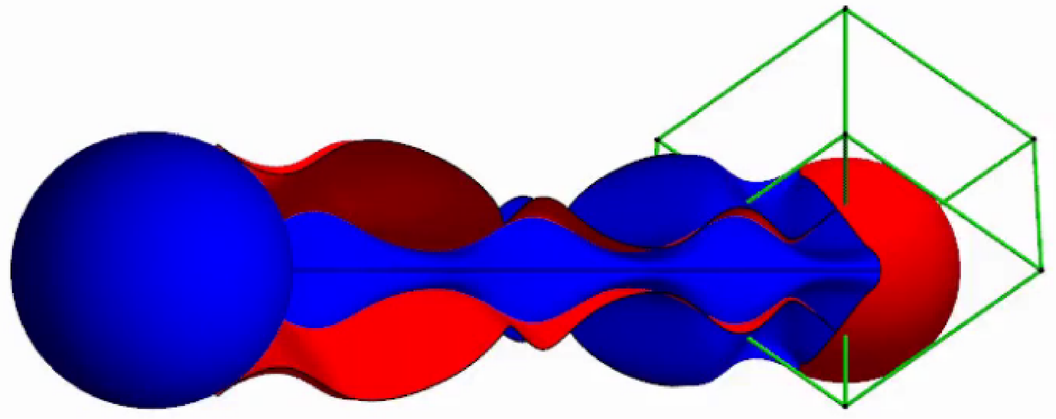

Closest grains from which manifolds originate that intersect transversally

In the BCC lattice:

$(\phi_\mathrm{f} = 0)$

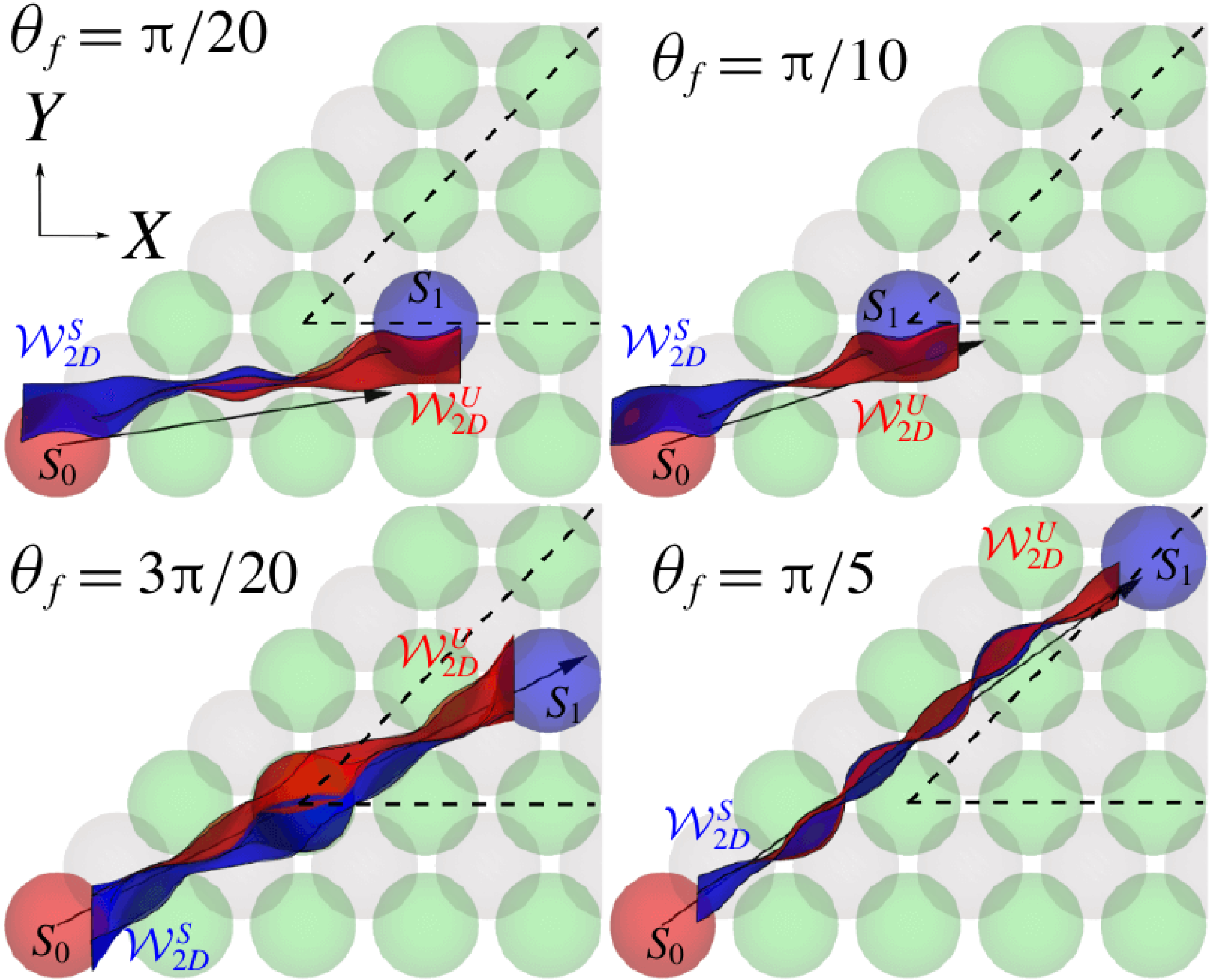

Predicting the relative variations of λ with the flow orientation

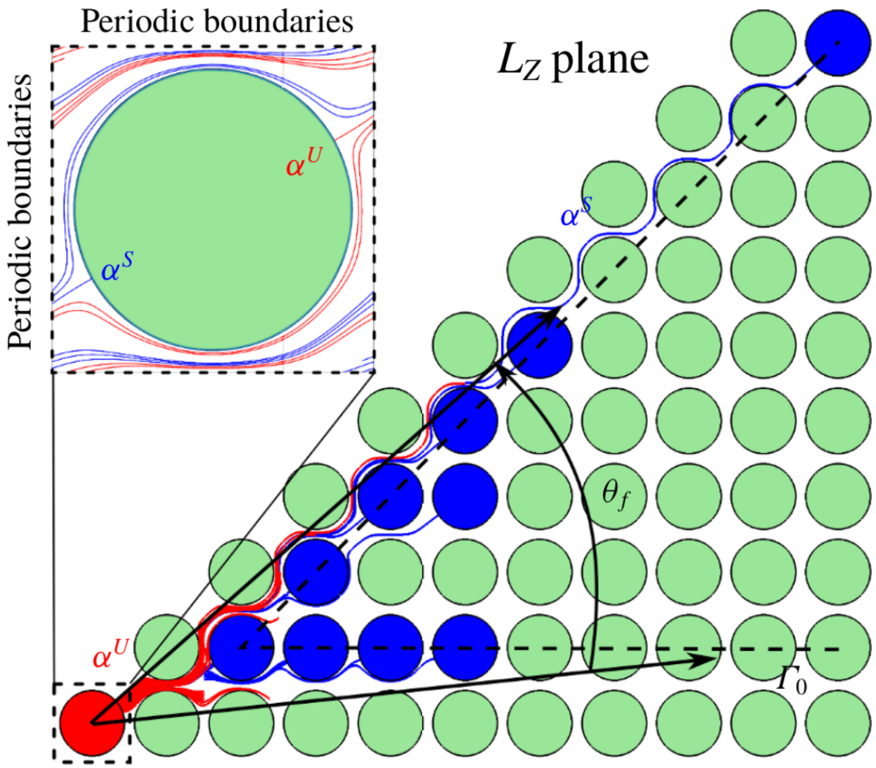

Turuban et al.
JFM 2019

$$\lambda\left(\theta_f\right) \propto \frac{1}{d\left(\theta_f\right)}$$ (empty circles)

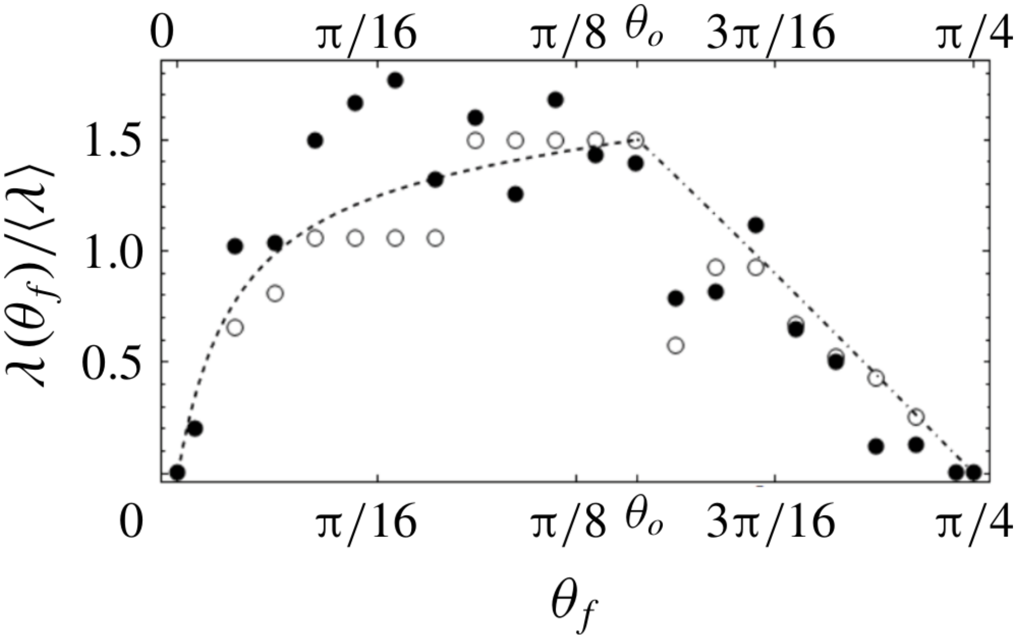

- What happens in a random porous medium ?
- To know it, we need an experiment

2) Chaotic advection in a random packing of monodisperse beads: An experimental study

Optical tomography

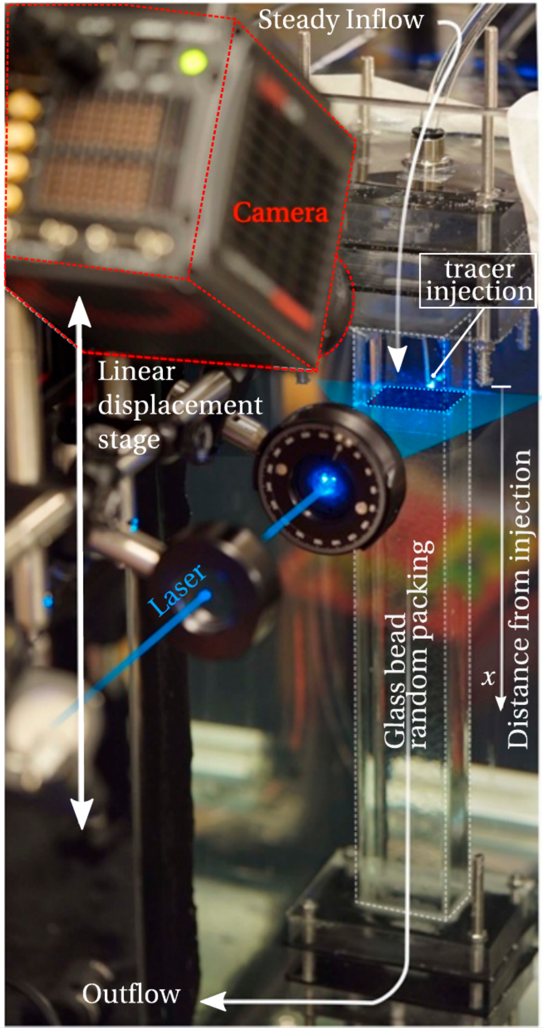

- Random glass bead packing
- The liquid is a glycerol-water mixture whose refractive index is matched to that of the beads
- **Steady flow** through the column from top to bottom
- A fluorescent dye is continuously injected at the top through a needle (5 mm diameter) → **Steady solute plume**
- Laser-induced fluorescence → visualization in a horizontal plane
- The laser sheet can be moved vertically
- The camera moves with the laser sheet

→ Measurement of the 3D concentration field

$$\mathrm{Re} = ud/\nu \approx 5 \cdot 10^{-3} \ll 1$$

$$\mathrm{Pe} = u\ \mathrm{d}/\mathrm{D_m} \approx 8.6 \cdot 10^{3}$$

Heyman et al. (PNAS 2020)

18 experiments with 3 beads sizes (7, 10, 20 mm)

Observation in horizontal planes as a function of distance to injection

Raw data

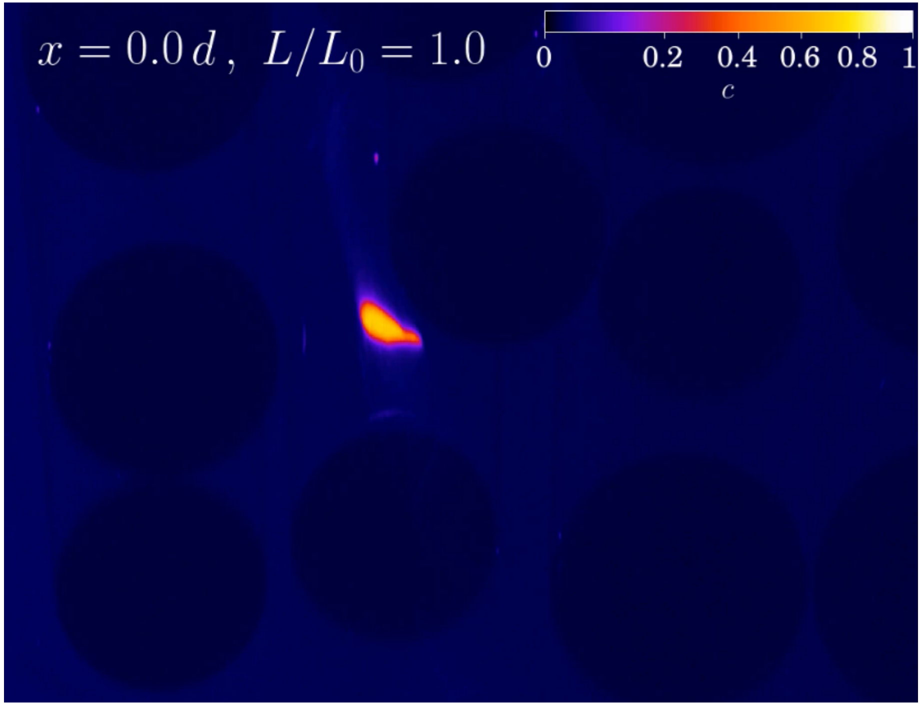

Observation in horizontal planes as a function of distance to injection

Raw data

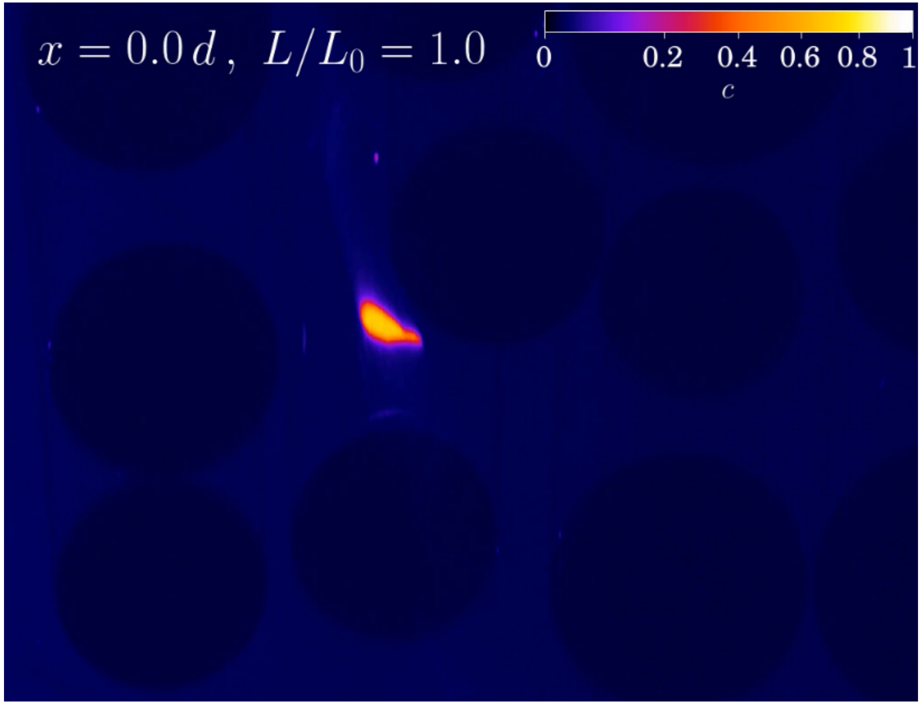

Heyman et al. (PNAS 2020)

Filament and elongation inferred from spline fitting

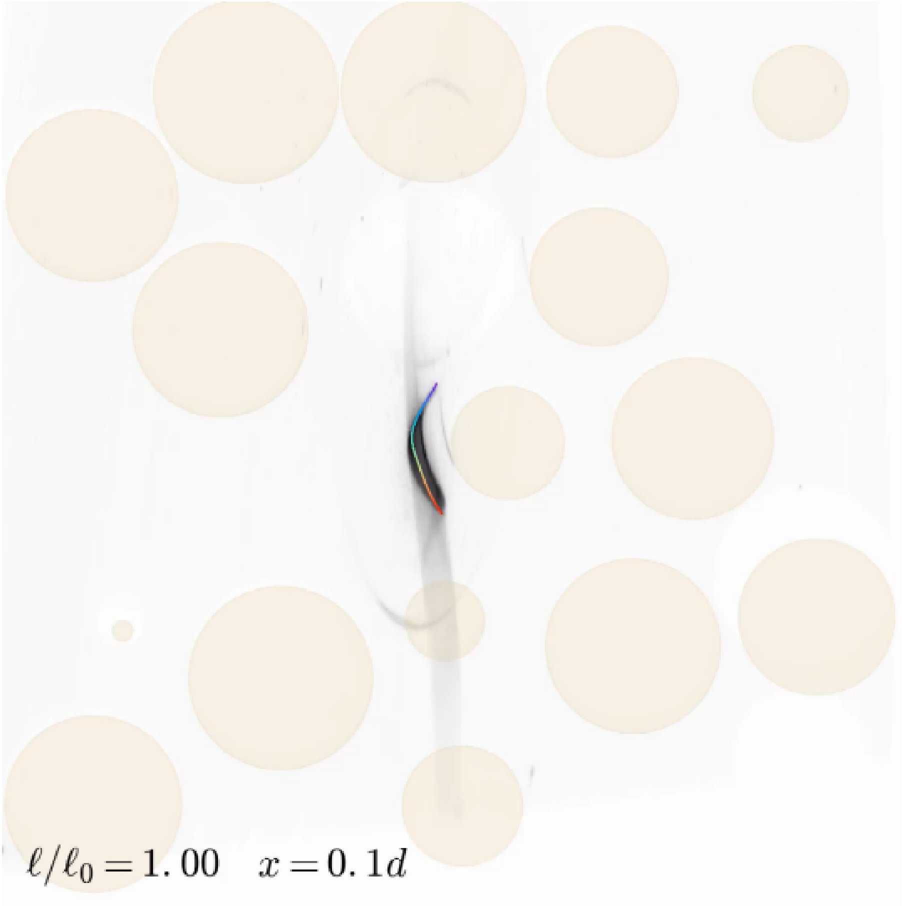

Exponential stretching of material lines

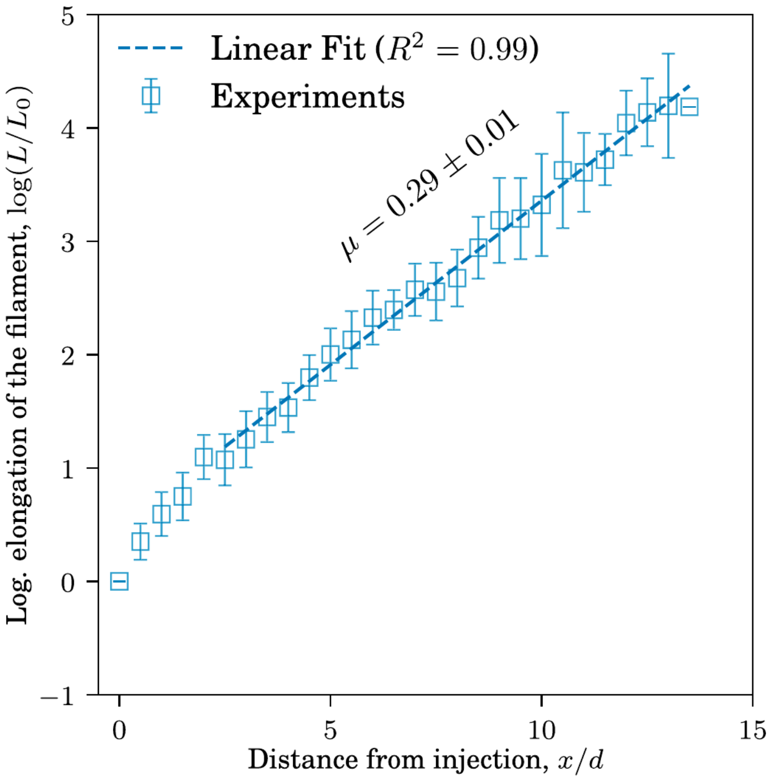

Heyman et al. (PNAS 2020)

$$\mu = \ln\left(L/L_0\right)/(x/d) = 0.29 \pm 0.01$$

= Topological entropy of the flow (independent of bead diameter and flow rate)

For a fluid element of lenth l :

Results from the product of successive random stretching events with rates distributed according to a distribution of mean λ and variance $\sigma_\lambda^2/2$

→ $\log(l)$ goes to a normal distribution and l to a log-normal distribution of mean

$$\langle l \rangle \sim \exp\left(\mu x/d\right) \quad \text{with} \quad \mu = \lambda + \sigma_\lambda^2/2$$

Phenomenology of folding

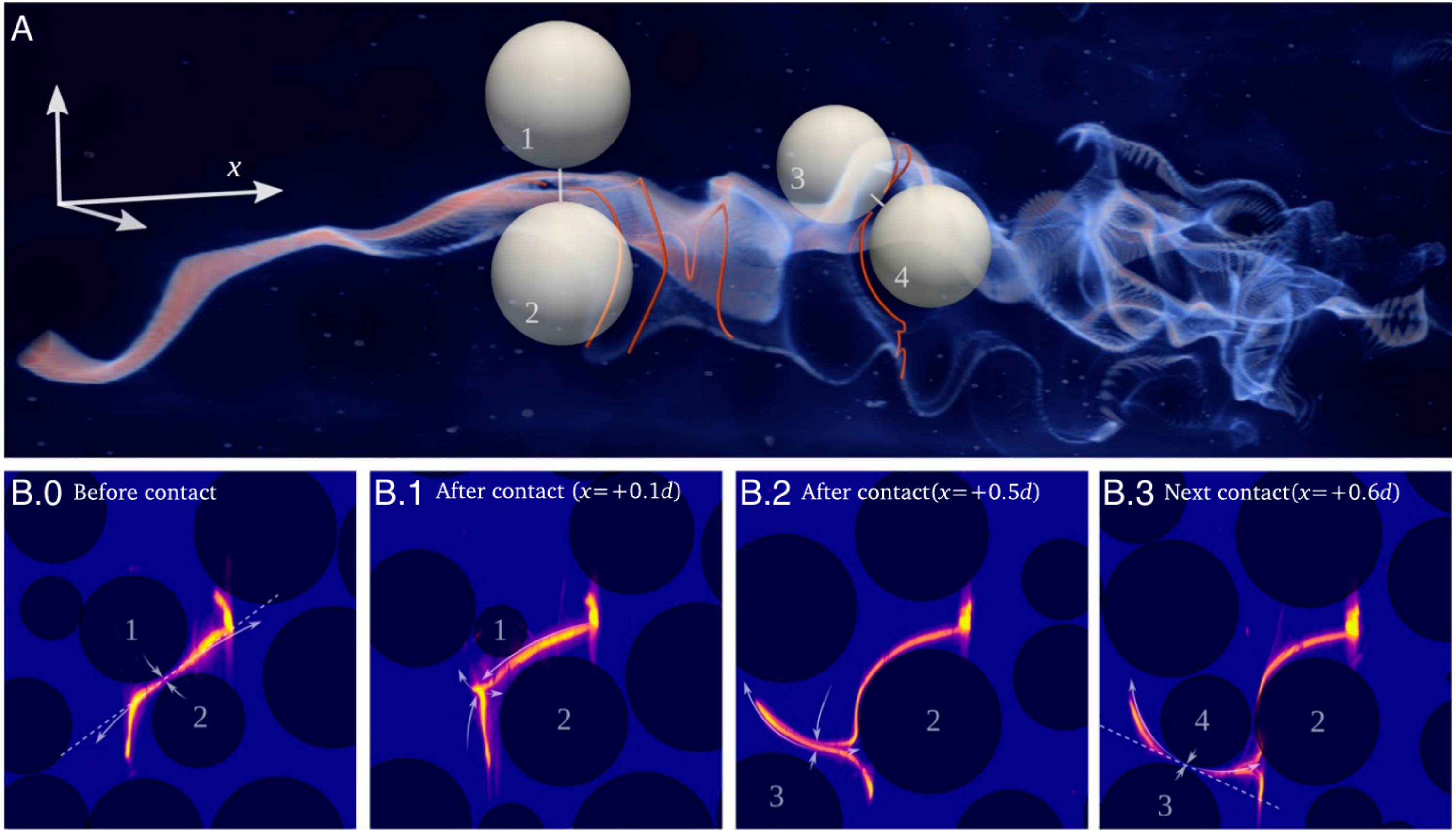

Exchange between the directions of compression and stretching when the fluid element passes through a contact between grains.

Linking the stretching statistics to the porous geometry

n_c = number of cusps along the filament

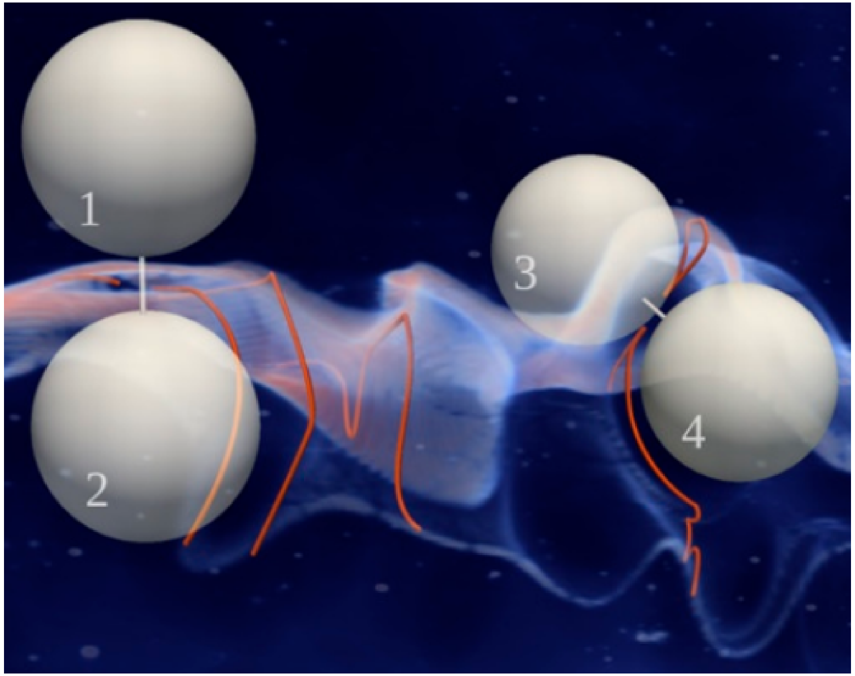

$L_c = L/n_c$ = mean segment length

S_c = mean area swept by a segment

Average distance between two successive contact points through which the solute sheet goes:

$$X_c = S_c/L_c \approx 3.45d$$

Linking the stretching statistics to the porous geometry (2)

n_c = number of cusps along the filament

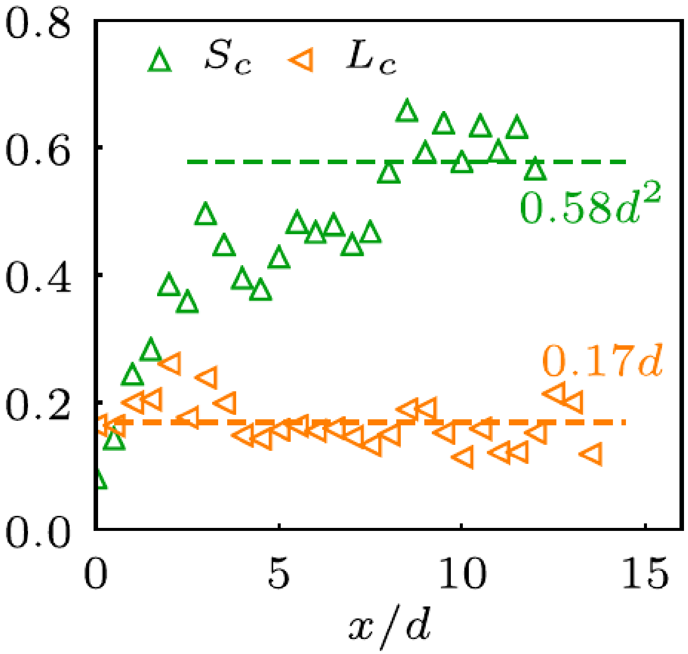

$L_c = L/n_c$ = mean segment length

S_c = mean area swept by a segment

Average distance between two successive contact points through which the solute sheet goes:

$$X_c = S_c/L_c \approx 3.45d$$

The filament length doubles at each of these events, so

$$\ell(X) = 2^{(X/X_c)} \quad \text{and} \quad \lambda \equiv \frac{\mathrm{d}(\log \ell)}{\mathrm{d}(X/d)} = \frac{\log 2}{X_c/d} \approx 0.21$$

In an isotropic packing, we can show that $X_c \approx 8\log 2\phi z_c d_p/3$

→ The Lyapunov exponent can be predicted as

$$\boxed{\lambda \approx \tfrac{3}{8}\tfrac{\phi z_c d_p}{d}} = 0.27$$

Heyman et al. (PNAS 2020)

Predicting the Lyapunov (with prefactor) in the ordered packings

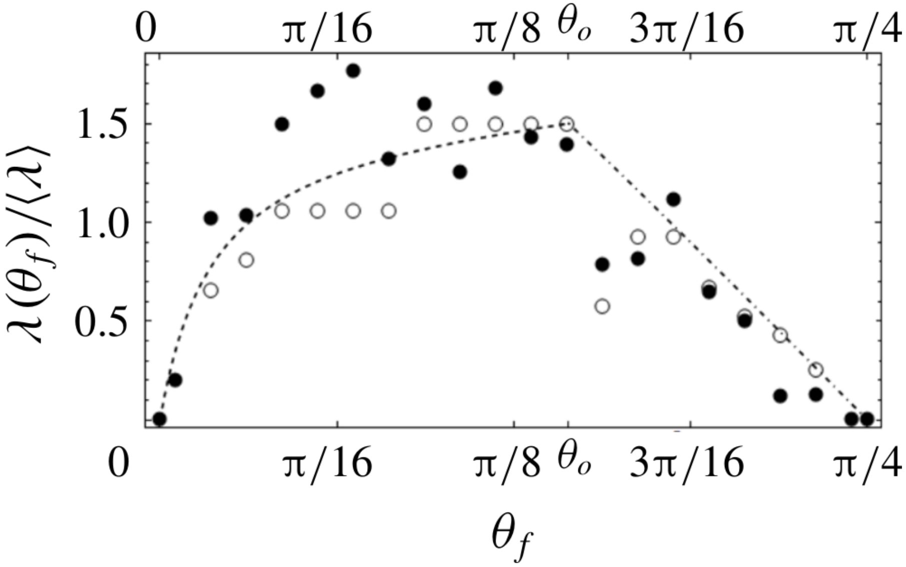

Using the previous theoretical prediction:

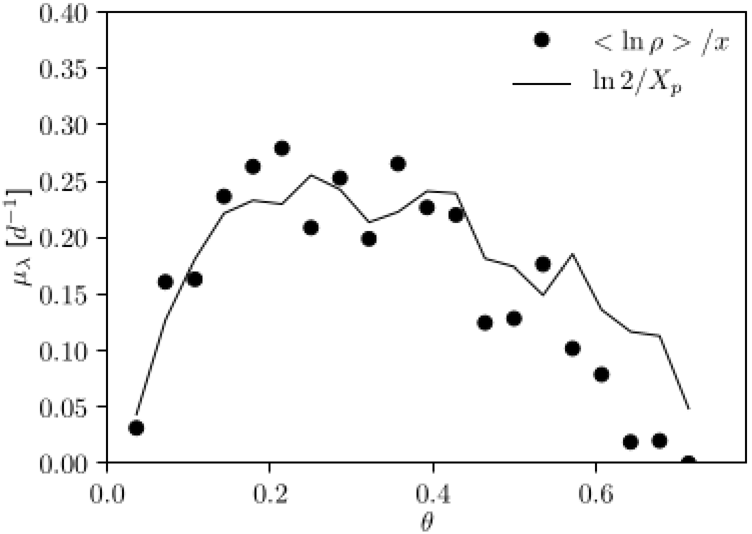

Lester et al., in preparation (2022)

→ Good agreement !

Consequences for solute mixing

Length scale below which the diffusive spreading rate of the solute manages to homogenize solute concentrations against the compression rate of fluid:

$$\frac{D_\mathrm{m}}{s_\mathrm{B}^2} > \frac{u}{d} \Longrightarrow \frac{s_\mathrm{B}}{d} < \frac{1}{\sqrt{\lambda Pe}}$$ (Batchelor’s scale)

Hence: $\frac{s_\mathrm{B}}{d} < 1 \Longrightarrow Pe > 5$ → Value smaller than that met in most cases in most natural and industrial porous media

→ Incomplete pore scale mixing is the rule rather than the exception:

- Altered effective chemical kinetics and microbioal growth dynamics
- Conventional models cannot manage to predict the associated mixing (e.g., decrease in the maximal concentration)
- The lamellar mixing model can (not shown here)

→ Porous media are excellent mixers/stirrers:

$$\eta = \frac{\lambda u/d}{\mathbf{e}}$$

Average stretching rate

Average strain rate

$\eta \simeq 3\%$ (industrial mixers: 3%, microfluidic mixers: 0.3 to 0.4%)

Conclusions, papers

Conclusions:

- Advective mixing associated to Stokes flow is intrinsically chaotic in all types of random porous media
- We explained the mechanism for chaotic injection
- The associated Lyapunov can be predicted
- Consequently solutes are badly-mixed at the pore scale for most configurations of practical use

Papers:

- R. Turuban, D. R. Lester, T. Le Borgne & Y. Méheust (2018), Space-Group Symmetries Generate Chaotic Fluid Advection in Crystalline Granular Media, *Phys. Rev. Lett.* **120**, 024501.
- R. Turuban, D. R. Lester, H. Heyman, T. Le Borgne & Y. Méheust (2019), Chaotic Mixing in Crystalline Granular Media, *J. Fluid Mech.* **871**, 562-594.
- J. Heyman, D. R. Lester, R. Turuban, Y. Méheust & T. Le Borgne (2020), Stretching and folding sustain microscale chemical gradients in porous media., *Proc. Nat. Acad. Sci.* **117** (24), 13359-13365.
- D. Lester, J. Heyman, Y. Méheust & T. Le Borgne (2024), A unified theory of chaotic mixing in porous media: from pore networks to granular systems, in preparation.
- M. Souzy, H. Lhuissier, Y. Méheust, T. Le Borgne & B. Metzger (2020), Velocity distributions, dispersion and stretching in three-dimensional porous media, *J. Fluid Mech.* **891**, A16.

Collaborators & funding

Collaborators:

Régis Turuban

Joris Heyman

Tanguy Le Borgne

Géosciences Rennes

Daniel Lester
RMIT, Melbourne Australia

Funding:

- University Rennes 1 (PhD grant, Y. Méheust)
- CPER “Tranport by flows” (Y. Méheust)
- ERC “ReactiveFronts” (T. Le Borgne)

Environmental context

- Flow and reactive transport processes in continental systems:
  - Regional flow patterns driven by topography, precipitations and outflow boundary conditions (surface waters)
  - Recharge of aquifers occurs through the vadose (unsaturated) zone
  - Strong spatial heterogeneity of the subsurface

    → complex mixing interfaces (f.e. oxygen-richand anoxic water) that are hot spots for biological/chemical activity
  - At the pore scale, interaction between solutes, minerals and micro-organisms

    → precipitation, dissolution, adsorption, redox reactions

→ What happens at very small scales impacts large-scale geochemical fluxes

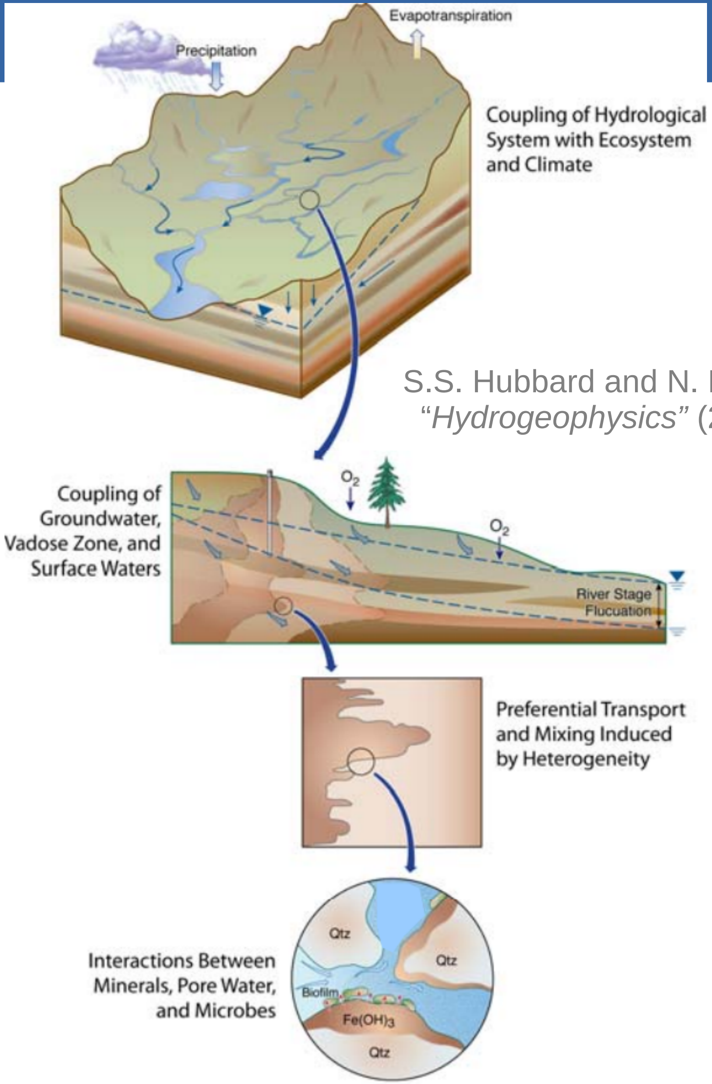

S.S. Hubbard and N. Linde, "*Hydrogeophysics*" (2011)

Mixing of solutes in subsurface water : a crucial process (2)

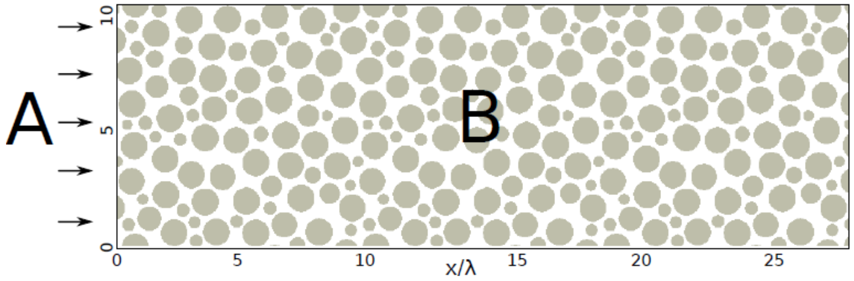

$$A + B \longrightarrow C$$

(High Damköhler)

Chemo-luminescent reaction → local reaction rate

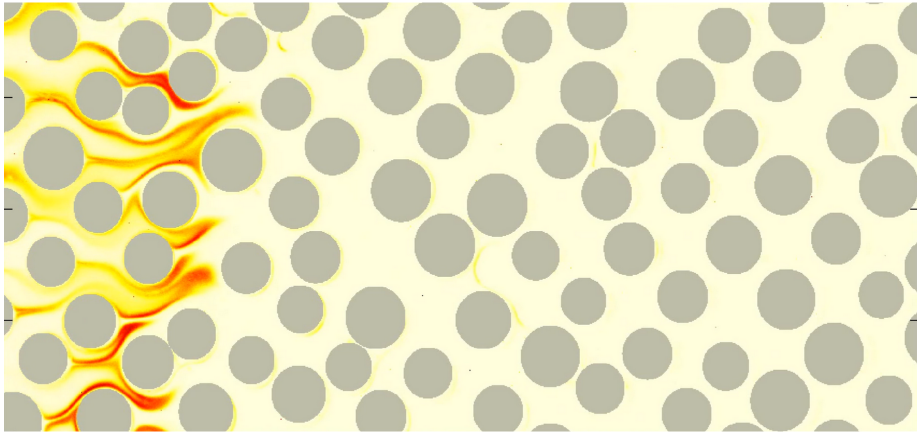

Which processes and concepts are we studying ?

- **Solute transport:**
  - Advection displaces the solutes with the local flow velocity
  - Molecular diffusion tends to homogenize the solutes' concentration fields

Péclet number: $$Pe = \frac{t_{\mathrm{diff}}}{t_{\mathrm{adv}}} = \frac{U\,L}{D_{\mathrm{m}}}$$

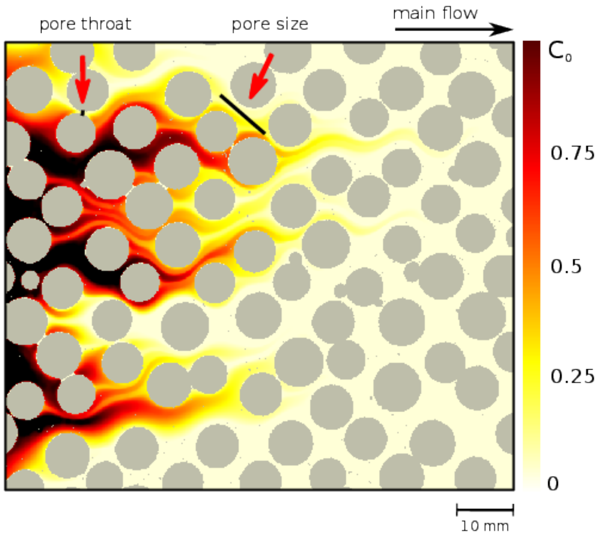

- **Reactive transport:**

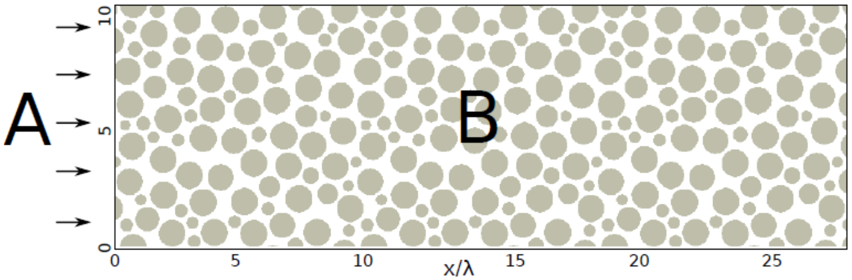

$$A + B \longrightarrow C$$

Damköhler number: $$\mathcal{D}a = \frac{\tau_{\mathrm{a}}}{\tau_{\mathrm{r}}} = \frac{l/\bar{v}}{1/(c_0\,k)} = \frac{l\,c_0\,k}{\bar{v}}$$

(well-mixed conditions ↔ low Damköhler)

- **Dispersion/spreading:**

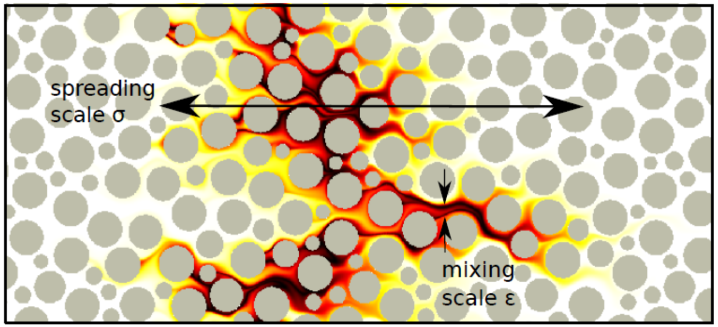

Modelling the mixing dynamics under linear shear

- Model based on the stretching lamella:

$$\frac{1}{s(t)}\frac{ds}{dt} = \frac{D_{\rm eff}}{s(t)^2} - \frac{1}{l(t)}\frac{dl}{dt} \qquad (1)$$

(compression-diffusion equation)

Ranz, AIChE J. (1979); Villermaux & Duplat, PRL (2003)

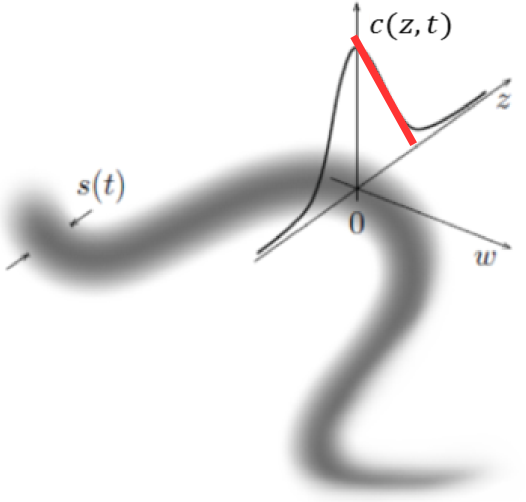

- Here we assume that stretching can be modeled by simple linear shear:

$$\frac{l(t)}{l_0} = \rho(t) = \sqrt{1+\overline{\nabla v}^2\, t^2} \sim_{t\to\infty} \overline{\nabla v}\, t$$

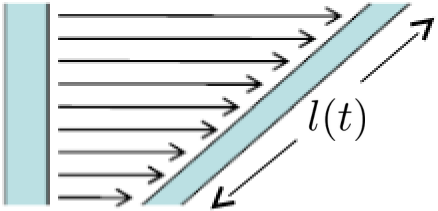

- In this case the solution of Eq. (1) is a Gaussian profile with maximum:

$$c_{\rm m}(t) = \frac{c_0}{\sqrt{1+4\,\tau_{\rm e}(t)}} \qquad (2)$$

with $\tau_{\rm e}(t) = \frac{D_{\rm eff}}{s_0^2}\int_0^t dt\ \rho(t)^2$ (warped time) $D_{\rm eff}$ = effective diffusion coefficient

At large *t*: $c_{\rm m}(t) \sim \frac{s_0}{\overline{\nabla v}\sqrt{D_{\rm eff}\, t^3}}$

- The mean concentration gradient in the fingers can be simply estimated as: $$\overline{\nabla c}(t) = \frac{c_{\rm m}(t)}{\overline{s}(t)} \qquad (3)$$
- For linear shear: $$\overline{s}(t) \approx \sqrt{\frac{s_0^2}{1+\overline{\nabla v}^2 t^2} + 2\,D_{\rm eff}\, t} \qquad (4)$$

Le Borgne et al, JFM (2015)

Modelling the mixing dynamics under linear shear (2)

$$\chi_\Omega(t) = D\left(\overline{\nabla c}^2(t) + \xcancel{\sigma^2_{\nabla c}(t)}\right)$$ (5)

$$(2) + (3) + (4) + (5) \Longrightarrow \boxed{\overline{\chi}_\Omega(t) = \frac{D}{\frac{s_0^2}{1+\overline{\nabla v}^2 t^2} + 2D_{\text{eff}}t}\,\frac{c_0^2}{1+4\tau_{\text{e}}(t)}}$$

Why does the BCC lattice generate much more chaos than the SC lattice ?

Additional glide symmetries in the BCC:

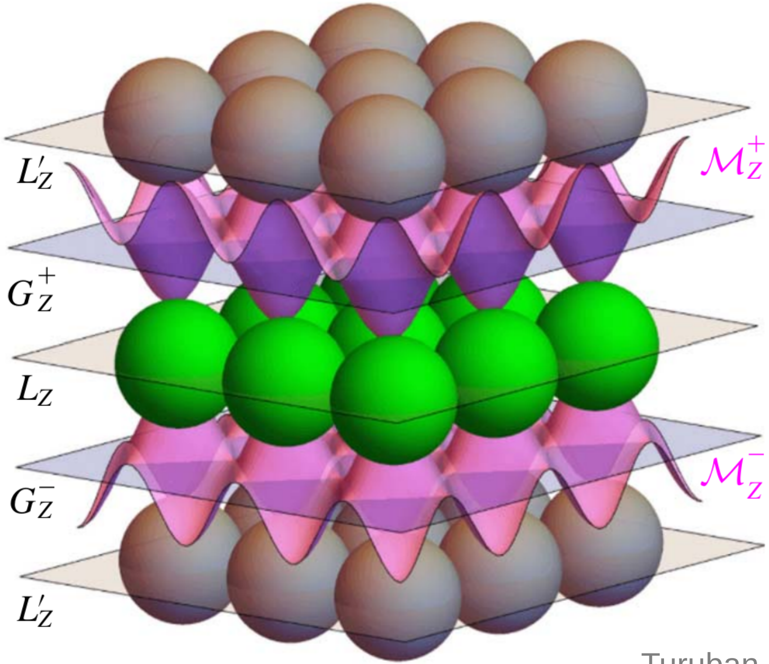

Turuban et al.
(PRL, 2018, JFM 2019)

The associated material surfaces constrain the manifolds:

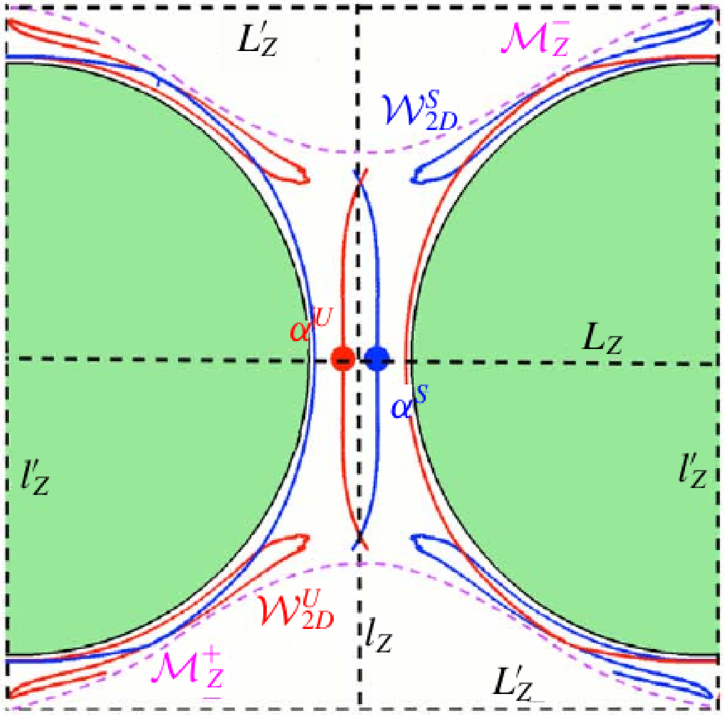

→ This particular example contradicts the general assertion according to which “more symmetry means that chaos is less likely”

Predicting the relative variations of the Lyapunov with the flow orientation (2)

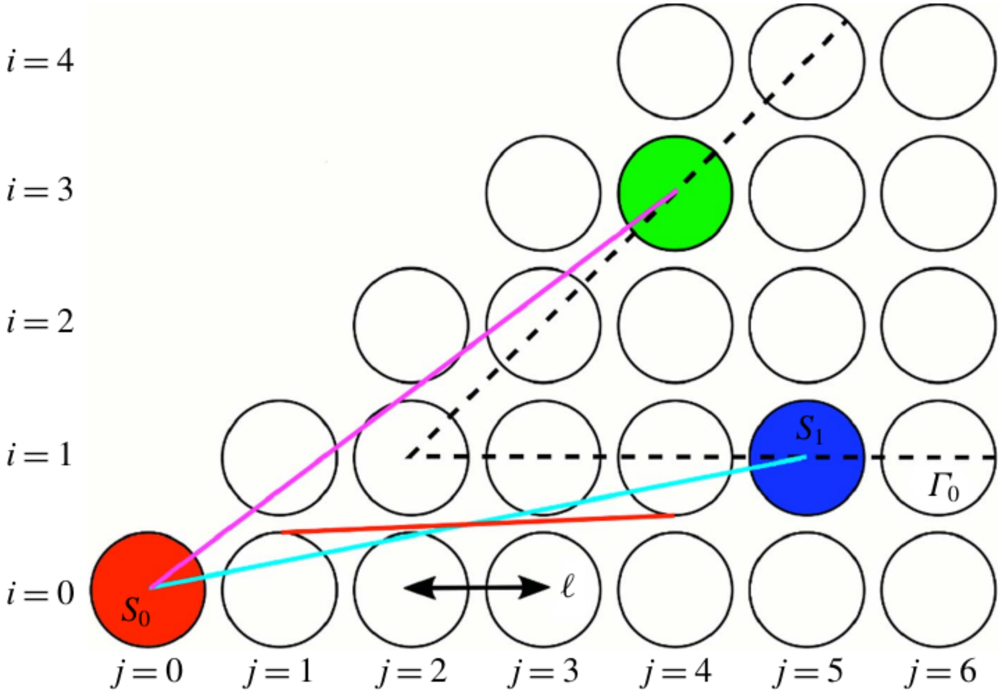

Turuban et al.
JFM 2019

$$\lambda\left(\theta_f\right) \propto \frac{1}{d\left(\theta_f\right)}$$ (empty circles)

Geometric estimate:

$$d\left(\theta_f\right) = \begin{cases} \ell\sqrt{1+\left(2+\cot\theta_f-\frac{2}{\ell}\csc\theta_f\right)^2} & \\ \frac{\ell}{\cos\theta_f-\sin\theta_f} & \text{for } \theta_o \leqslant \theta_f \leqslant \frac{\pi}{4} \end{cases}$$